International Research Journal of Innovations in Engineering and Technology (IRJIET)

ISSN (online): 2581-3048
Volume 10, Issue 6, pp 255-261, June-2026
https://doi.org/10.47001/IRJIET/2026.106032

Effect of Filler Electrode Selection on the Corrosion Rate of AISI 304 Stainless Steel Welded by Gas Tungsten Arc Welding

[1]*Ahmad Mafruchul Fitroh, [2]Agus Suprihanto, [3]Ojo Kurdi

[1,2,3]Department of Mechanical Engineering, Universitas Diponegoro, Semarang, Indonesia
*Corresponding Author's E-mail: mafruchulfitroh@gmail.com

***Abstract* - AISI 304 austenitic stainless steel (SS304) is widely used in the chemical, food, petrochemical, energy, and marine industries due to its excellent mechanical properties, corrosion resistance, and weldability. However, the thermal cycles generated during welding can alter the microstructure of the weld metal and heat-affected zone (HAZ), thereby affecting the mechanical properties and corrosion resistance of welded joints. This study aimed to investigate the effects of E308L, E309L, and E316L filler electrodes on the microstructure, mechanical properties, and corrosion resistance of SS304 joints produced by the Gas Tungsten Arc Welding (GTAW) process. Welding was performed at a constant current of 130 A, an arc voltage of 12–14 V, and pure argon shielding gas. Mechanical properties were evaluated through tensile testing in accordance with ASTM E8 and Vickers hardness testing based on ASTM E384. Microstructural observations were conducted using optical microscopy, while corrosion resistance was assessed by potentiodynamic polarization testing according to ASTM G61. The results showed that all weld metals were predominantly composed of the austenitic phase with varying amounts of δ-ferrite. The E308L electrode produced a relatively fine dendritic structure with a moderate δ-ferrite content, whereas E309L resulted in a higher δ-ferrite fraction and a coarser dendritic structure. The E316L electrode produced a more homogeneous austenitic structure due to the presence of molybdenum (Mo). The highest tensile strength was obtained with the E308L electrode (561.40 MPa), followed by E316L (561.38 MPa), while E309L exhibited the lowest tensile strength (502.63 MPa). The highest elongation was achieved by E316L (16.35%). Furthermore, E316L exhibited the lowest corrosion rate of 0.000474 mm/year, indicating superior corrosion resistance. Overall, the E316L electrode provided the most favorable combination of mechanical properties and corrosion resistance for GTAW welding of SS304 stainless steel.**

Keywords: AISI 304 Stainless Steel, GTAW, Filler Electrode, Microstructure, Mechanical Properties, Corrosion Resistance.

I. INTRODUCTION

AISI 304 austenitic stainless steel (SS304) is one of the most widely used engineering materials in the chemical, food-processing, energy, petrochemical, and marine industries owing to its excellent combination of mechanical properties, superior corrosion resistance, and outstanding fabrication and weldability characteristics [1], [2]. The corrosion resistance of SS304 is primarily attributed to the formation of a chromium-rich passive oxide film (Cr_2O_3) on its surface, which effectively inhibits oxidation and protects the material from aggressive corrosive environments. Nevertheless, under certain service conditions, particularly after welding, the mechanical properties and corrosion resistance of SS304 may deteriorate due to microstructural modifications occurring in the weld metal and heat-affected zone (HAZ) [3]. Figure 1 illustrates corrosion damage observed in an AISI 304 welded joint used in a seawater cooler pipeline system.

Figure 1: Seawater Cooler Pipe

The welding process involves repeated heating and cooling cycles, which may promote recrystallization, alloying element segregation, chromium carbide precipitation, and variations in the distribution of δ-ferrite and austenite phases within the weld metal [1], [4]. These microstructural transformations significantly influence the mechanical properties of welded joints, including tensile strength, hardness, and ductility, and may increase their susceptibility to intergranular and localized corrosion [2], [5]. Therefore, the quality and performance of SS304 welded joints are strongly

International Research Journal of Innovations in Engineering and Technology (IRJIET)

ISSN (online): 2581-3048

Volume 10, Issue 6, pp 255-261, June-2026

https://doi.org/10.47001/IRJIET/2026.106032

affected by welding parameters, among which the selection of filler metal plays a crucial role [4].

ER308L, ER309L, and ER316L filler electrodes possess different chemical compositions, resulting in distinct weld metal characteristics. ER308L has a chemical composition similar to that of AISI 304 stainless steel and is therefore commonly employed for welding austenitic stainless steels of the 304 grade. In contrast, ER309L contains higher chromium and nickel contents, which promote δ-ferrite formation and reduce the susceptibility to hot cracking during weld solidification [4], [6]. Meanwhile, ER316L contains molybdenum (Mo), which is known to enhance resistance to pitting and crevice corrosion, particularly in chloride-containing environments [6]. Consequently, the differences in chemical composition among these filler electrodes are expected to produce variations in phase constitution and weld metal microstructure, which ultimately affect the mechanical properties and corrosion resistance of the welded joints [7].

Several previous studies have investigated the effects of welding parameters and filler metal selection on the mechanical and corrosion properties of austenitic stainless steels. Chuaiphan and Srijaroenpramong [6] reported that different filler metals resulted in significant variations in microstructure and corrosion behavior of stainless steel welded joints. Similarly, Akgül [3] demonstrated that filler metal selection substantially influenced the microstructure, hardness, and corrosion characteristics of AISI 304L welded joints. Other studies have also revealed that variations in filler metal composition during Gas Tungsten Arc Welding (GTAW) alter the δ-ferrite content and consequently affect the mechanical properties of the weld metal [1]. However, studies specifically comparing the effects of ER308L, ER309L, and ER316L filler electrodes in similar GTAW welding of SS304 remain limited, particularly with respect to correlating microstructural evolution with mechanical properties and corrosion rate. Such information is essential for determining the most suitable filler electrode to achieve an optimum combination of mechanical performance and corrosion resistance in SS304 welded joints.

Therefore, the present study aims to investigate the influence of ER308L, ER309L, and ER316L filler electrodes on the microstructure, mechanical properties, and corrosion rate of GTAW-welded SS304 stainless steel joints. Mechanical characterization was carried out through tensile and hardness tests, while corrosion resistance was evaluated using the potentiodynamic polarization method. The findings of this study are expected to provide scientific insights and practical recommendations regarding the selection of appropriate filler electrodes for SS304 applications operating in environments susceptible to corrosion.

II. METHODOLOGY

2.1 Research Design

This study employed an experimental approach to investigate the effect of ER308L, ER309L, and ER316L filler electrodes on the mechanical properties, microstructure, and corrosion rate of austenitic stainless steel SS304 welded joints. The independent variable was the type of filler electrode, namely ER308L, ER309L, and ER316L. The dependent variables included hardness, tensile strength, microstructure, and corrosion rate. Meanwhile, the controlled variables comprised the base material, joint design, welding position, welding current, arc voltage, shielding gas, and other welding parameters to ensure that the observed differences in weld characteristics were primarily attributed to variations in filler metal composition.

2.2 Specimen Preparation

The base material used in this study was AISI 304 austenitic stainless steel (SS304) in plate form. In general, SS304 contains 18–20 wt.% chromium (Cr), 8–10.5 wt.% nickel (Ni), a maximum carbon content of 0.08 wt.%, manganese up to 2 wt.%, silicon up to 1 wt.%, phosphorus up to 0.045 wt.%, sulfur up to 0.03 wt.%, with the balance being iron (Fe). The presence of chromium and nickel provides a stable austenitic microstructure and promotes the formation of a chromium-rich passive oxide film (Cr_2O_3), which is responsible for the excellent corrosion resistance of the material.

The SS304 plates were machined using a CNC milling machine according to the dimensions required for welding and subsequent testing. A butt joint configuration with a single V-groove and a groove angle of 60° was employed. Prior to welding, the specimen surfaces were thoroughly cleaned using abrasive paper and acetone to remove oil, dust, and oxide layers in order to minimize contamination that could adversely affect weld quality. The geometry and dimensions of the specimens used for corrosion testing, hardness measurements, and microstructural observations are illustrated in Figure 2.

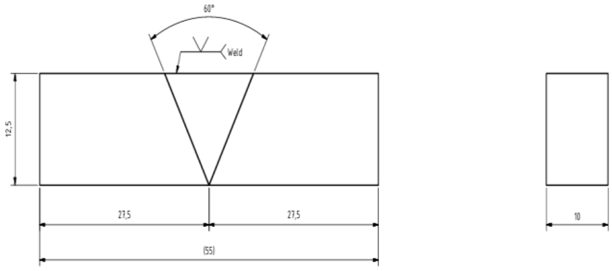

Figure 2: Geometry and Dimensions of Specimens for Corrosion Testing, Hardness Measurement, and Microstructural Observation

ISSN (online): 2581-3048
Volume 10, Issue 6, pp 255-261, June-2026
https://doi.org/10.47001/IRJIET/2026.106032

2.3 Welding Procedure

Welding was performed using the Gas Tungsten Arc Welding (GTAW) process with direct current and Direct Current Electrode Negative (DCEN) polarity. Tungsten electrodes of EWTh-2 or EWCe-2 type with a diameter of 2.4 mm were used. Pure argon gas (99.99%) served as the shielding gas at a flow rate ranging from 10 to 12 L/min.

Three types of filler electrodes, namely ER308L, ER309L, and ER316L, each with a diameter of 2.4 mm, were employed. All welding operations were carried out in the flat position under constant welding conditions, with a welding current of 130 A and an arc voltage of 12–14 V. Maintaining constant welding parameters was intended to ensure that any differences in weld characteristics could be mainly attributed to the effect of filler electrode composition.

2.4 Preparation of Test Specimens

Tensile testing specimens were prepared in accordance with ASTM E8/E8M standards. The specimens were machined using a CNC milling machine such that the welded joint was located at the center of the gauge length. Tensile tests were conducted using a Universal Testing Machine to determine the ultimate tensile strength (UTS), yield strength, and percentage elongation.

Microhardness measurements were performed using the Vickers method in accordance with ASTM E384. Indentations were made in the weld metal, heat-affected zone (HAZ), and base metal regions. Multiple indentation points were applied in each region to obtain the average hardness values and hardness distribution across the welded joint.

2.5 Microstructural Observation

Microstructural characterization was carried out using an optical metallurgical microscope. Samples were sectioned transverse to the welding direction and subsequently subjected to mounting, sequential grinding using abrasive papers up to 2000 grit, polishing with alumina paste, and chemical etching using a suitable reagent for austenitic stainless steel. The observations were conducted to identify grain morphology, phase distribution of austenite and δ-ferrite, as well as microstructural changes occurring in the weld metal and heat-affected zone.

2.6 Corrosion Testing

Corrosion behavior was evaluated using the potentiodynamic polarization method in accordance with ASTM G61. A three-electrode corrosion testing system was employed, consisting of the specimen as the working electrode, an Ag/AgCl electrode as the reference electrode, and a platinum plate as the counter electrode. The tests were conducted in a chloride-containing corrosive medium to determine the corrosion potential (Ecorr), corrosion current density (Icorr), and corrosion rate.

2.7 Data Analysis

The tensile test data were processed to determine the average values of ultimate tensile strength, yield strength, and percentage elongation for each filler electrode variation. Hardness data were analyzed in terms of hardness distribution profiles across the base metal, heat-affected zone, and weld metal regions.

Microstructural observations were qualitatively evaluated by comparing grain size, dendritic morphology, and the distribution of austenite and δ-ferrite phases among the different filler electrodes. Furthermore, the relationship between microstructural evolution, mechanical properties, and corrosion resistance was comprehensively assessed.

The corrosion parameters, namely corrosion potential (Ecorr) and corrosion current density (Icorr), were used to calculate the corrosion rate. Finally, the experimental results obtained for ER308L, ER309L, and ER316L filler electrodes were comparatively analyzed to determine the influence of filler electrode selection on the microstructure, mechanical properties, and corrosion resistance of SS304 welded joints, as well as to identify the electrode providing the optimum overall welding performance.

III. RESULTS AND DISCUSSION

3.1 Microstructure of SS304 Weld Joints

The microstructural observations show that all SS304 weld joints using E308L, E309L, and E316L electrodes are predominantly composed of the austenite (γ) phase with the presence of δ-ferrite in the weld metal region. The fraction and distribution of δ-ferrite are influenced by the chemical composition of the filler metal, particularly Cr, Ni, and Mo contents, which subsequently affect the mechanical properties and corrosion resistance of the welded joints [8].

In the weld joint produced using the E308L electrode, the weld metal consists of an austenitic matrix with approximately 3–10% δ-ferrite. As shown in Figure 3(a), the presence of δ-ferrite reduces the tendency for hot cracking because ferrite has a higher solubility for sulfur and phosphorus compared to austenite, thereby reducing impurity segregation at grain boundaries during solidification [9]. In addition, the relatively homogeneous distribution of δ-ferrite produces a finer dendritic structure, resulting in higher tensile strength and hardness [10].

ISSN (online): 2581-3048
Volume 10, Issue 6, pp 255-261, June-2026
https://doi.org/10.47001/IRJIET/2026.106032

(a)

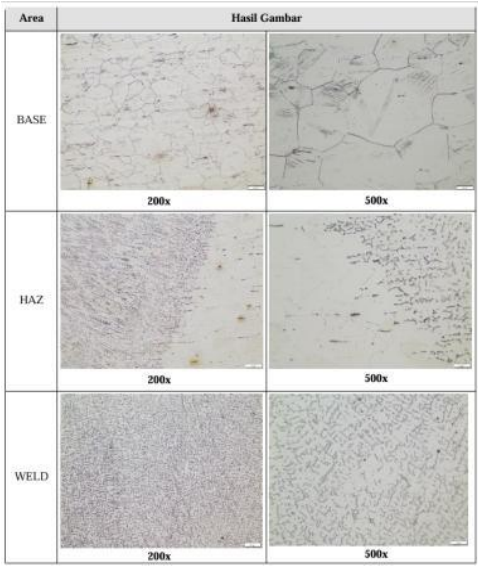

(b)

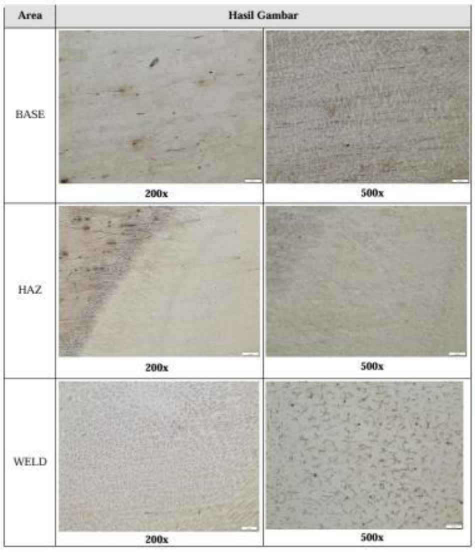

(c)

Figure 3: Microstructure of weld joints using electrodes (a) E308L, (b) E309L, and (c) E316L

For the E309L electrode, the higher Cr (23–25%) and Ni (12–14%) contents promote greater δ-ferrite formation in the weld metal, as shown in Figure 3(b). The increased δ-ferrite fraction improves solidification stability and reduces the risk of hot cracking [1]. However, the coarser dendritic structure and less uniform ferrite distribution increase microstructural heterogeneity, which reduces ductility and the mechanical performance of the weld joint [6].

Meanwhile, the E316L electrode produces a microstructure dominated by austenite with a lower amount of δ-ferrite and a finer ferrite distribution, as shown in Figure 3(c). The presence of approximately 2–3% molybdenum (Mo) enhances the stability of the Cr_2O_3 passive layer and accelerates repassivation after local damage occurs. This condition results in superior corrosion resistance compared to E308L and E309L [11].

Overall, a finer and more homogeneous microstructure leads to more uniform stress distribution, improved ductility, and enhanced mechanical properties and corrosion resistance of welded joints [12].

3.2 Effect of Electrode on Tensile Properties

Tensile testing was conducted using a Universal Testing Machine. Each variable was tested three times. The results are presented in Table 1.

International Research Journal of Innovations in Engineering and Technology (IRJIET)

ISSN (online): 2581-3048

Volume 10, Issue 6, pp 255-261, June-2026

https://doi.org/10.47001/IRJIET/2026.106032

Table 1: Tensile Test Results (ASTM E8)

Specimen	Area (mm^2)	Tensile Strength (MPa)	Elongation (%)	Peak Force (N)
308 L	91.699	561.398	14.180	51399.922
309 L	90.492	502.627	9.731	45783.980
316 L	87.313	561.378	16.345	48922.108

The ASTM E8 tensile test results indicate that E308L and E316L electrodes produce nearly identical maximum tensile strengths, at 561.40 MPa and 561.38 MPa, respectively, while E309L shows a lower tensile strength of 502.63 MPa.

The highest elongation value was obtained with E316L at 16.35%, followed by E308L at 14.18%, and E309L at 9.73%. The relatively high tensile strength of E308L is influenced by the combination of an austenitic matrix and a moderate amount of δ-ferrite, which produces a finer structure and hinders dislocation movement [9].

In contrast, the coarser microstructure and non-uniform ferrite distribution in E309L lead to reduced tensile strength and ductility. This condition is attributed to higher local stress concentration and reduced plastic deformation capability [6].

For E316L, the presence of Mo promotes solid solution strengthening in the austenitic matrix without significantly reducing ductility. The more homogeneous austenitic structure also results in more uniform stress distribution, thereby improving plastic deformation capability [13]. Therefore, E316L provides the best combination of strength and ductility.

3.3 Effect of Electrode on Vickers Hardness

Vickers hardness testing was performed using a Vickers Hardness Tester. Each variable was tested three times. The results are presented in Table 2.

Table 2: Vickers Hardness Test Results (ASTM E384)

Specimen	Base (HVN)	HAZ (HVN)	Weld (HVN)
308 L	236.000	190.835	194.500
309 L	234.485	189.500	166.985
316 L	254.500	193.985	192.500

The hardness distribution shows that all specimens experienced a decrease in hardness in the heat-affected zone (HAZ) compared to the base metal. The reduction in HAZ hardness ranges from 19–24%. This phenomenon is caused by the thermal cycle during welding, which leads to grain coarsening, stress relieving, and a reduction in dislocation density. According to the Hall–Petch relationship, an increase in grain size reduces the number of grain boundaries that act as barriers to dislocation motion, thereby decreasing material strength and hardness [12]. Similar observations have been reported in austenitic stainless steel welds, where HAZ hardness decreases due to grain growth during welding [14].

In the weld metal region, the E308L electrode exhibits the highest hardness value of 194.50 HV, followed by E316L at 192.50 HV and E309L at 166.99 HV. The higher hardness of E308L is attributed to the formation of a relatively fine austenite and δ-ferrite structure [15]. In contrast, the higher Ni content in E309L increases austenite phase stability, resulting in a more ductile structure with lower hardness [1].

3.4 Effect of Electrode on Corrosion Resistance

Potentiodynamic polarization testing shows that the corrosion rate of SS304 weld joints is strongly influenced by the type of electrode used, as presented in Table 3.

Table 3: Corrosion Rate Test Results (ASTM G102)

Specimen	Potential (mV)	Current Density (μA/cm^2)	Corrosion Rate (mm/year)
E308L	196.7367	0.06272467	0.00057713
E309L	207.5400	0.07386767	0.00067966
E316L	189.4400	0.05150500	0.00047389

The E316L electrode exhibits the lowest corrosion current density (Icorr) of 0.05151 μA/cm^2 and the lowest corrosion rate of 0.000474 mm/year. In contrast, E309L shows the highest Icorr value of 0.07387 μA/cm^2 with a corrosion rate of 0.000680 mm/year, while E308L produces a corrosion rate of 0.000577 mm/year.

The superior corrosion resistance of E316L is attributed to the presence of Mo, which enhances the stability of the Cr_2O_3 passive film and accelerates repassivation after localized damage (He *et al.,* 2020). Molybdenum also increases the Pitting Resistance Equivalent Number (PREN), thereby improving resistance to pitting corrosion in chloride-containing environments (Varmaziar *et al.,* 2022). In contrast, the coarser dendritic structure and non-uniform δ-ferrite distribution in E309L may form microgalvanic cells between austenite and ferrite, accelerating metal dissolution and increasing the corrosion rate [6]. Nevertheless, all specimens exhibit corrosion rates below 0.001 mm/year, which are classified as excellent corrosion resistance for stainless steel materials in chloride-containing environments [16].

ISSN (online): 2581-3048
Volume 10, Issue 6, pp 255-261, June-2026
https://doi.org/10.47001/IRJIET/2026.106032

3.5 Relationship Between Microstructure, Mechanical Properties, and Corrosion Resistance

The differences in mechanical properties and corrosion resistance of SS304 weld joints are primarily influenced by variations in microstructure formed due to different filler electrodes. A moderate amount of δ-ferrite in E308L provides a good balance between strength and hardness. A higher δ-ferrite content in E309L improves solidification stability but produces a more heterogeneous structure, leading to reduced mechanical properties and corrosion resistance. In contrast, the austenite-dominant structure and the presence of Mo in E316L result in a more homogeneous microstructure, improved ductility, and the best corrosion resistance [9].

Therefore, the E316L electrode provides the most optimal combination of properties for SS304 welding, as it achieves high tensile strength, the highest elongation, and the lowest corrosion rate compared to E308L and E309L.

IV. CONCLUSIONS

Based on the results of the study on the effect of E308L, E309L, and E316L welding electrodes on the microstructure, mechanical properties, and corrosion rate of GTAW-welded joints in austenitic stainless steel SS304, the following conclusions can be drawn:

1. The microstructure of all welded joints is dominated by the austenitic phase with the presence of δ-ferrite in the weld metal region. The E308L electrode produces an austenitic structure with a moderate amount of δ-ferrite and relatively fine dendritic morphology. The E309L electrode results in a higher δ-ferrite fraction and a coarser dendritic structure, whereas the E316L electrode produces a more homogeneous austenitic structure with a lower amount of δ-ferrite and contains molybdenum (Mo), which enhances the stability of the passive layer.
2. The tensile properties of the weld joints are strongly influenced by the resulting microstructural characteristics. The E308L and E316L electrodes yield the highest tensile strengths, at 561.40 MPa and 561.38 MPa, respectively, while the E309L electrode exhibits the lowest tensile strength of 502.63 MPa. The highest elongation is achieved by the E316L electrode at 16.35%, followed by E308L at 14.18% and E309L at 9.73%, indicating that E316L provides the best ductility.
3. Vickers hardness distribution shows a reduction in hardness in the HAZ due to the thermal welding cycle, which leads to grain growth and stress relief. In the weld metal region, the E308L electrode produces the highest hardness value of 194.50 HV, followed by E316L at 192.50 HV, while E309L shows the lowest hardness of 166.99 HV.
4. Corrosion resistance is influenced by passive film stability and microstructural homogeneity. The E316L electrode exhibits the lowest corrosion current density (Icorr) and corrosion rate, at 0.05151 µA/cm² and 0.000474 mm/year, respectively, indicating the best corrosion resistance. The E308L electrode shows a corrosion rate of 0.000577 mm/year, while the E309L electrode exhibits the highest corrosion rate of 0.000680 mm/year. However, all specimens fall below 0.001 mm/year, indicating excellent corrosion resistance.

Overall, the E316L electrode provides the most optimal performance for SS304 welding, as it delivers the best combination of high tensile strength, superior ductility, and the highest corrosion resistance. The E308L electrode offers a balanced combination of strength and hardness, whereas the E309L electrode shows relatively lower mechanical performance and corrosion resistance compared to the other electrodes.

Research Implications

The selection of welding electrodes for SS304 should be tailored to service conditions. The E316L electrode is more suitable for applications operating in chloride-containing or corrosive environments, such as chemical processing equipment, petrochemical systems, and marine structures. In contrast, the E308L electrode may be considered for applications prioritizing joint strength and hardness under less aggressive environmental conditions.

REFERENCES

[1] G. Lothongkum, E. Viyanit, and P. Bhandhubanyong, "Study on the effects of pulsed TIG welding parameters on delta-ferrite content, shape factor and bead quality in orbital welding of AISI 316L stainless steel plate," *J. Mater. Process. Technol.*, vol. 110, no. 2, pp. 233–238, 2001, doi: 10.1016/S0924-0136(00)00875-X.

[2] H. T. Serindağ and G. Çam, "Multi-pass butt welding of thick AISI 316L plates by gas tungsten arc welding: Microstructural and mechanical characterization," *Int. J. Press. Vessel. Pip.*, vol. 200, no. October, pp. 13–16, 2022, doi: 10.1016/j.ijpvp.2022.104842.

[3] O. AKGÜL and A. B. BAŞYİĞİT, "Investigating the Microstructural Properties and Phase Distributions of TIG Welded AISI/SAE 304L Stainless Steel Runners in TNT Filled Ammunutions," *Uluslararası Muhendis. Arastirma ve Gelistirme Derg.*, vol. 14, no. 1, pp. 228–236, 2022, doi: 10.29137/umagd.1015109.

[4] H. Shah Hosseini, M. Shamanian, and A. Kermanpur, "Characterization of microstructures and mechanical properties of Inconel 617/310 stainless steel dissimilar

ISSN (online): 2581-3048
Volume 10, Issue 6, pp 255-261, June-2026
https://doi.org/10.47001/IRJIET/2026.106032

welds," *Mater. Charact.*, vol. 62, no. 4, pp. 425–431, 2011, doi: 10.1016/j.matchar.2011.02.003.

[5] P. Marashi, M. Pouranvari, S. Amirabdollahian, A. Abedi, and M. Goodarzi, "Microstructure and failure behavior of dissimilar resistance spot welds between low carbon galvanized and austenitic stainless steels," *Mater. Sci. Eng. A*, vol. 480, no. 1–2, pp. 175–180, 2008, doi: 10.1016/j.msea.2007.07.007.

[6] W. Chuaiphan, P. Kumkoon, and P. Kalnaowakul, "Dissimilar welding of AISI 201 and 202 low nickel stainless steels by GTA and PA welding processes," *J. Alloy. Metall. Syst.*, vol. 4, no. November, p. 100047, 2023, doi: 10.1016/j.jalmes.2023.100047.

[7] M. M. Soleymani and H. Mostafaei, "The effect of filler metal on the mechanical behavior of stainless steel welded by GTAW welding," vol. 11, no. 4, pp. 38–55, 2024, doi: 10.22034/IJME.2024.458059.1961.

[8] J. Andersson, "Welding metallurgy and weldability of superalloys," 2020. doi: 10.3390/met10010143.

[9] J. C. Lippold, Welding Metallurgy and Weldability of Stainless Steels. *John Wiley & Sons, Inc., Hoboken, New Jersey*.

[10] K. Z. Ghumman, S. Ali, E. U. Din, A. Mubashar, N. B. Khan, and S. W. Ahmed, "Experimental investigation of effect of welding parameters on surface roughness, micro-hardness and tensile strength of AISI 316L stainless steel welded joints using 308L filler material by TIG welding," *J. Mater. Res. Technol.*, vol. 21, pp. 220–236, 2022, doi: 10.1016/j.jmrt.2022.09.016.

[11] J. Xiejun, G. Wan, Y. L. Yuan, and Y. Gao, "Corrosion behavior of 316L stainless steel weld under constant strain," *J. Phys. Conf. Ser.*, vol. 1653, no. 1, 2020, doi: 10.1088/1742-6596/1653/1/012035.

[12] W. D. Callister and D. Rethwisch, *Materials Science and Engineering*. 2014.

[13] A.Mahajan, H. Singh, S. Kumar, and S. Kumar, "Mechanical properties assessment of TIG welded SS 304 joints," *Mater. Today Proc.*, vol. 56, pp. 3073–3077, 2022, doi: 10.1016/j.matpr.2021.12.133.

[14] H. Ming, Z. Zhang, J. Wang, E. H. Han, and W. Ke, "Microstructural characterization of an SA508-309L/308L-316L domestic dissimilar metal welded safe-end joint," *Mater. Charact.*, vol. 97, pp. 101–115, 2014, doi: 10.1016/j.matchar.2014.08.023.

[15] A.Karpagaraj, J. A. S. Edberk, T. D. B. Kannan, D. K. Rajendran, and T. Ramesh, "Effect of GTAW process parameters on joining stainless steel 316L," *AIP Conf. Proc.*, vol. 2460, no. August, 2022, doi: 10.1063/5.0095789.

[16] Fontana. M. G, *Corrosion Engineering*. 1986.

Citation of this Article:

Ahmad Mafruchul Fitroh, Agus Suprihanto, & Ojo Kurdi. (2026). Effect of Filler Electrode Selection on the Corrosion Rate of AISI 304 Stainless Steel Welded by Gas Tungsten Arc Welding. *International Research Journal of Innovations in Engineering and Technology - IRJIET*, 10(6), 255-261. Article DOI https://doi.org/10.47001/IRJIET/2026.106032

****